Desalination and Water Treatment
www.deswater.com
doi: 10.1080/19443994.2014.991760

57 (2016) 4028–4036
February

Taylor & Francis
Taylor & Francis Group

Removal of heavy metals from aqueous solution using Fe_3O_4 nanoparticles coated with Schiff base ligand

Sheida Moradinasab, Mahdi Behzad*

Department of Chemistry, Semnan University, Semnan 35351-19111, Iran, Tel. +98 23 33383195; Fax: +98 23 33654110; emails: mbehzad@semnan.ac.ir, mahdibehzad@gmail.com (M. Behzad)

Received 15 June 2014; Accepted 18 November 2014

ABSTRACT

Fe_3O_4 magnetic nanoparticles modified with Schiff base ligand were prepared to remove heavy metal ions from aqueous solutions. The structure, optical properties, and morphology of the as-synthesized Fe_3O_4@SiO_2/Schiff base ligand were investigated by powder X-ray diffraction technique, FT-IR, and scanning electron microscopy. Experiments showed that Fe_3O_4@SiO_2/Schiff base ligand nanoadsorbent can be effectively used to remove Cu(II), Zn(II), and Ni(II) ions from water. Fe_3O_4@SiO_2/Schiff base ligand nanoparticles could be separated by external magnet after adsorption process. Adsorption equilibrium was achieved in 60 min and maximum removal of metal ions was obtained at pH 5. The isotherm analyses indicated that the adsorption data better fitted to the Langmuir isotherm model. The maximum adsorption capacities were 97.2, 87, and 81.6 mg g^{-1} for Cu(II), Zn(II), and Ni(II), respectively. In addition, adsorption kinetic data followed a pseudo-second-order rate for three tested metal ions.

Keywords: Fe_3O_4@SiO_2/Schiff base ligand; Adsorption; Isotherm models; Heavy metals

1. Introduction

Heavy metals are among the important factors that have polluted environment [1]. In the past decades, many hazards of several heavy metal ions such as lead, cadmium, nickle, chromium, copper, and zinc have been discovered [2]. The development of new adsorbents with improved adsorption characteristics has remained as a significant research objective for the environmental pollution control processes [3]. Heavy metals can easily enter the food chain through a number of pathways. These metal ions can cause progressive toxic effects with gradual accumulation in living organisms [4]. The main techniques, which have been utilized to reduce the heavy metals content of effluents, include chemical precipitation [5], ion exchange [6,7], adsorption [8–10], membrane processes [11,12], and electrolytic methods [13]. The especial properties of nanoparticles have provided unprecedented opportunities for the adsorption of heavy metals ions in highly efficient and economical approaches [14]. Recently, much attention has been focused on surface functionalized magnetic nanoparticles. These nanosized magnetic particles are considered potential adsorbents for aqueous heavy metals due to their high surface area and the unique advantage of easy separation under external magnetic fields [15–17]. Schiff bases are prepared from the condensation of amino and carbonyl compounds and are considered as an important class of ligands that coordinate to metal

*Corresponding author.

ions via azomethine nitrogen and have been studied extensively [18]. In azomethine derivatives, the C=N linkage is essential for biological activity; several azomethines were reported to possess remarkable antibacterial, antifungal, anticancer, and diuretic activities [19]. Schiff base complexes are considered to be among the most important stereochemical models in main group and transition metal coordination chemistry, thanks to their preparative accessibility and structural variety [20]. Another characteristic of the Schiff base ligands, which is currently under investigation, is their ability in the water treatment processes [21,22]. The interest in this ability of the Schiff bases comes from the fact that these materials have multidentate coordination sites, which are well suited to coordinate to transition metals. The present study focuses on the preparation of Fe_3O_4@SiO_2/Schiff base ligand nanoparticles, and investigations into their efficiency as adsorbent for the removal of metal ions from aqueous solutions. The characterization of the modified NPs was carried out by scanning electron microscopy (SEM), fourier transform infrared (FT-IR) spectroscopy, and powder X-ray diffraction (XRD). The thermodynamics and kinetics aspects of the removal process were also studied.

2. Experimental setup

2.1. Instrumentation and chemicals

$FeCl_2{\cdot}4H_2O$ and $FeCl_3{\cdot}6H_2O$ were purchased from the Merck Chemical Company in high purity. 3-amino propyl (triethoxy), silane (APTES), salicylaldehyde, and tetraethoxysilane (TEOS) were purchased from Sigma-Aldrich Chemical Company. All the solvents were distilled, dried, and purified by standard procedures. Metal ions concentration was obtained using a Shimadzu atomic absorption AA-680 spectrophotometer.

2.2. Preparation of magnetite Fe_3O_4 nanoparticles

Naked Fe_3O_4 nanoparticles were prepared by chemical coprecipitation of Fe^{3+} and Fe^{2+} ions with a molar ratio of 2:1. Typically, $FeCl_3{\cdot}6H_2O$ (2.92 g, 10.8 mmol) and $FeCl_2{\cdot}4H_2O$ (1.07 g, 5.4 mmol) were dissolved in 100 mL deionized water at 75–80℃ under N_2 atmosphere and vigorous mechanical stirring (600 rpm). Then, 5 mL of 25% NH_4OH was added drop by drop with vigorous stirring to produce a black solid product immediately. The reaction continued for another 30 min and the mixture was cooled to room temperature. The black precipitate formed was isolated by magnetic decantation, exhaustively washed with double distilled water until neutrality, and then, washed with ethanol and, finally, dried under vacuum at 75–80℃ for 24 h.

2.3. Preparation of Fe_3O_4@SiO_2 core–shell

Fe_3O_4 (0.50 g) was dispersed in the mixture of ethanol (100 mL), ammonia solution (3 mL), and TEOS (1 mL). This solution was stirred mechanically for 24 h at room temperature. Then the product, Fe_3O_4@SiO_2, was separated by an external magnet, washed three times with deionized water and ethanol, and dried at 80℃ for 10 h.

2.4. Preparation of Fe_3O_4@SiO_2/APTES

Typically, 0.30 mg of the as-synthesized Fe_3O_4@SiO_2 nanoparticles was dispersed in a mixture of 250 mL ethanol and 5 mL water by sonication. APTES (120 μL) was then added, and the mixture was mechanically stirred under N_2 atmosphere for 7 h. The nanoparticles were isolated by magnetic decantation and purified by five cycles of redispersion in ethanol and magnetic decantation. The Fe_3O_4@SiO_2/APTES nanoparticles were finally dried at room temperature under vacuum.

2.5. Preparation of Fe_3O_4@SiO_2/Schiff base ligand

The obtained Fe_3O_4@SiO_2/APTES powder (2 g) was dispersed in 100 mL ethanol solution and then salicylaldehyde (54 μL) was added to the mixture. After mechanical agitation under N_2 atmosphere at 40℃ for 4 h, the suspended substance was separated with external magnet, then washed by ethanol for three times, and dried at room temperature under vacuum. Fig. 1 summarizes the procedure of the preparation of the adsorbent.

2.6. Adsorption experiments

The adsorbent-adsorbate system was established at ambient temperature and in batch mode using stock solutions. A comparative study of the adsorption of Cu(II), Zn(II), and Ni(II) on the adsorbents, Fe_3O_4@SiO_2/Schiff base ligand, at different pH values was studied. In the adsorption measurements, metal ions solutions of different concentrations (from 25 to 200 ppm) and pH of 1–8 were used. The desired pH was maintained using dilute $NaOH/HNO_3$ solutions. During the experiments, the system was continuously stirred and at the end of each experiment, the Fe_3O_4@SiO_2/Schiff base ligand was separated by an

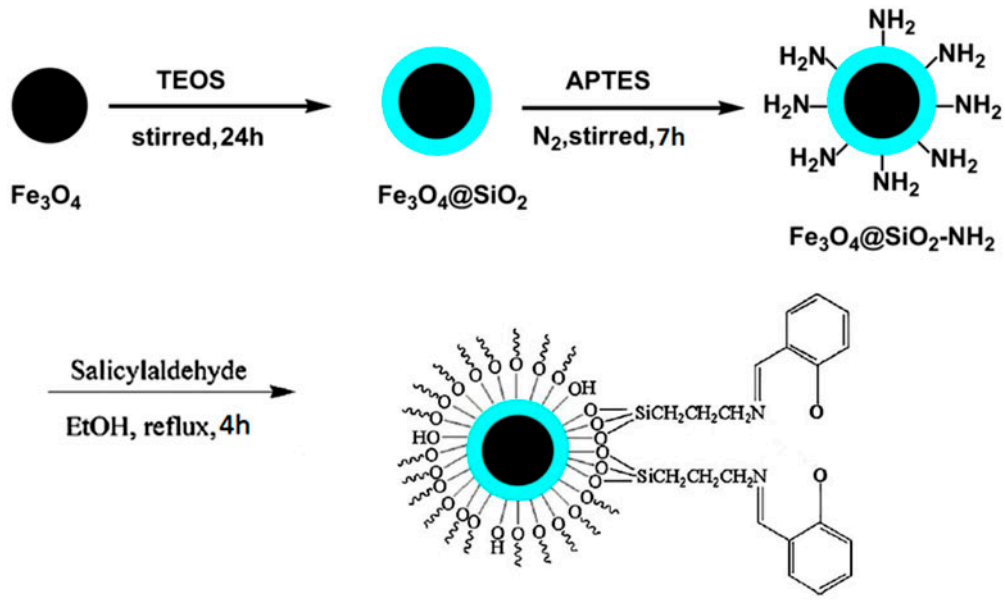

Fig. 1. Schematic representation of the synthesis of the adsorbent.

external magnet. The heavy metals removal percentage was calculated using Eq. (1).

$$\% \text{ Removal} = \left(\frac{C_0 - C_t}{C_0}\right) \times 100 \quad (1)$$

where C_0 (mg L^{-1}) and C_t (mg L^{-1}) are the metals concentration at initial and after time t, respectively, and the equilibrium adsorption capacity was calculated according to Eq. (2).

$$q_e = (C_0 - C_e)\ \frac{V}{W} \quad (2)$$

where C_0 (mg L^{-1}) and C_e (mg L^{-1}) are the initial and equilibrium metal ions concentrations in solution, respectively, V is the volume of the solution (L), and W is the mass (g) of the adsorbent.

2.7. Adsorption kinetics

In order to investigate the kinetics mechanism which controls the adsorption processes, such as mass transfer and chemical reaction, the pseudo-first-order and pseudo-second-order equations were applied to model the kinetics of metal ions adsorption onto Fe_3O_4@SiO_2/Schiff base ligand.

Eq. (3) shows the pseudo-first-order model, where K_1 is the rate constant of pseudo-first-order model (min^{-1}), q is the amount of metal ions adsorbed at various times (mg g^{-1}), and q_e is the amount of metal ions adsorbed on adsorbent at equilibrium (mg g^{-1}).

$$\log\ (q_e - q) = \log\ q_e - \left(\frac{K_1 t}{2.303}\right) \quad (3)$$

The pseudo-second-order model can be represented in the following form (Eq. (4)).

$$\frac{t}{q} = \frac{1}{(K_2 q_e)^2} + \frac{t}{q_e} \quad (4)$$

where K_2 is the rate constant of pseudo-second-order model (g (mg min)$^{-1}$).

2.8. Adsorption isotherms

The Langmuir equation is derived from simple mass action kinetic, assuming chemisorption. This model is based on two assumptions that the forces of interaction between adsorbed molecules are negligible and, once a molecule occupies a site, no further sorption takes place. The saturation value is reached beyond which no further sorption takes place.

This model, also called as the ideal localized monolayer model, is valid for monolayer sorption onto a surface with a finite number of identical sites, and is given by Eq. (5).

$$\frac{C_e}{q_e} = \frac{1}{q_m} C_e + \frac{1}{K_L q_m} \quad (5)$$

where q_m is a constant related to the area occupied by a monolayer of adsorbate, reflecting the maximum adsorption capacity (mg g^{-1}), C_e is the equilibrium liquid-phase concentration (mg L^{-1}), K_L is a direct measure of the intensity of adsorption (L mg^{-1}), and q_e is the amount adsorbed at equilibrium (mg g^{-1}).

From plotting $1/q_e$ vs. $1/C_e$, K_L, and q_m can be determined from the slope and intercept.

Freundlich adsorption isotherm, an adsorption isotherm, is a curve relating the concentration of a solute on the surface of an adsorbent to the concentration of the solute in liquid with which it is in contact. The linear form of Freundlich isotherm is:

$$\log q_e = \log K_F + \frac{1}{n} \log C_e \quad (6)$$

where K_F (L mg^{-1}) and n (dimensionless) is the heterogeneity factor. The values of n and K_F were calculated from the slope and intercept of the plot of log q_e vs. log C_e.

3. Results and discussion

3.1. Characterization of adsorbent

3.1.1. SEM

Fig. 2 shows the SEM image of Fe_3O_4@SiO_2/Schiff base ligand. The figure shows that the obtained material has a nearly porous structure which is suitable for adsorption studies.

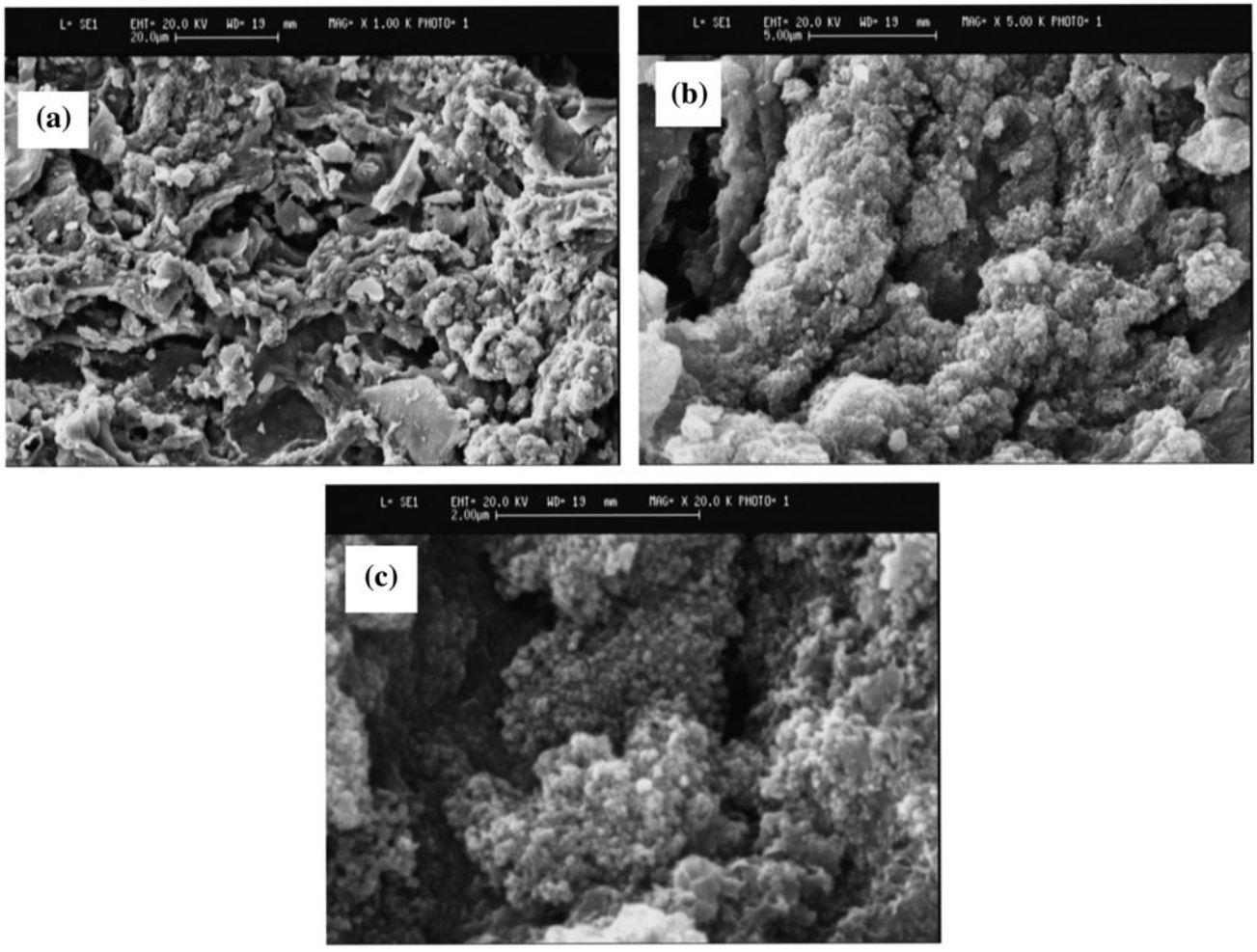

Fig. 2. SEM images of Fe_3O_4@SiO_2/Schiff base ligand with different magnifications.

3.1.2. FTIR

The FTIR spectrum of the pristine Fe_3O_4 is given in Fig. 3(A). A broad peak appeared around 3,350 cm^{-1} is due to the stretching vibration of the OH groups on the surface of Fe_3O_4 and the band observed at 574 cm^{-1} corresponds to the stretching vibrations of M_{Th}–O–M_{Oh}, where M_{Th} and M_{Oh} correspond to the iron occupying tetrahedral and octahedral positions, respectively.

FTIR spectra of Fe_3O_4@SiO_2/Schiff base ligand is shown in Fig. 3(B). The important peaks are characterized below. The broad peak appeared around 3,360 cm^{-1} could be assigned as the peak at similar region of the parent Fe_3O_4 nanoparticles and is due to the OH stretching of Fe_3O_4. The C=N stretching vibrations were observed at 1,627 cm^{-1}. A peak at 1,092 cm^{-1} was corresponded to Si–O (Fig. 4).

3.1.3. XRD

The structure of the Fe_3O_4@SiO_2/Schiff base ligand was determined by powder XRD. The pattern includes peaks at the 2θ: 30, 35, 43, 53, 57, and 62, which are assigned to h k l (2 2 0), (3 1 1), (4 0 0), (4 2 2), (5 1 1), and (4 4 5) (reference JCPDS 19-0629). For Fe_3O_4@SiO_2/Schiff base ligand nanoparticles, the broad peak was transferred to up angles due to the synergetic effect of amorphous silica and Schiff base ligand.

3.2. Effect of pH

The pH value of the solution is an important controlling parameter in the adsorption processes. The effect of pH on the adsorption of Cu(II), Zn(II), and Ni(II) onto Fe_3O_4@SiO_2/Schiff base ligand is shown in Fig. 5. As it could be seen from this figure, the removal efficiency was increased with increasing pH from 1.0 to 5.0, but changed little with increasing pH above 5.0. This could be easily rationalized by the fact that as the pH of the adsorption solution was lowered, the positive charges on the surface was increased. Therefore, it is clear that the decrease in the removal efficiency might be attributed to the repulsive forces between H^+ and the positive metal ions. We chose pH 5 for further experiments.

3.3. Effect of the amount of the adsorbent

The adsorption of the metal ions on Fe_3O_4@SiO_2/Schiff base ligand was studied by changing the quantity of the adsorbent in the range of 10–100 mg in 50 mL in the test solution, while keeping the initial metal ions concentration at 100 ppm. The removal percentage was found to increase with increase in the dosage of adsorbent. This is due to the availability of larger surface area with more active sites. Hence, the optimum dosage of the adsorbent to remove Cu(II), Zn(II), and Ni(II) was found to be 50 mg. The results are summarized in Fig. 6.

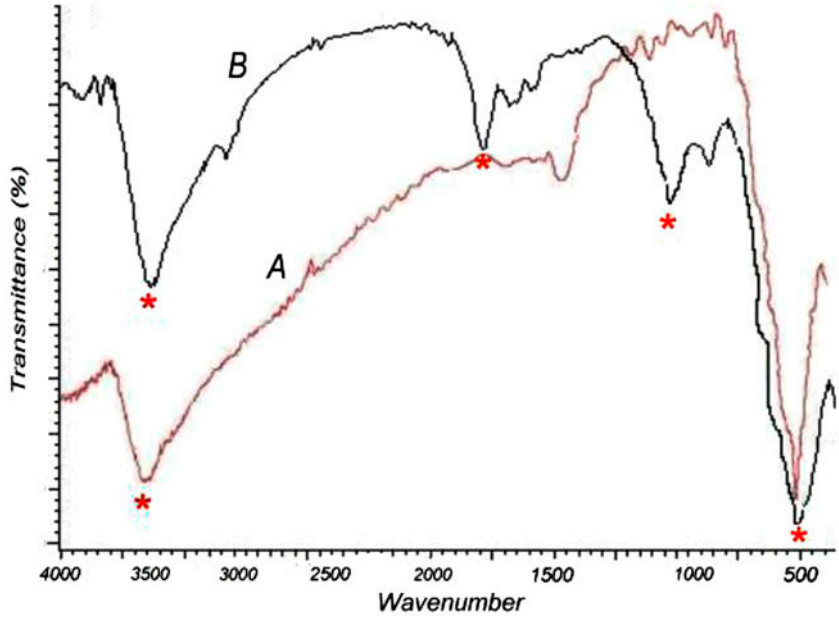

Fig. 3. Fourier transform-infrared analysis of (A) Fe_3O_4 and (B) Fe_3O_4@SiO_2/Schiff base ligand.

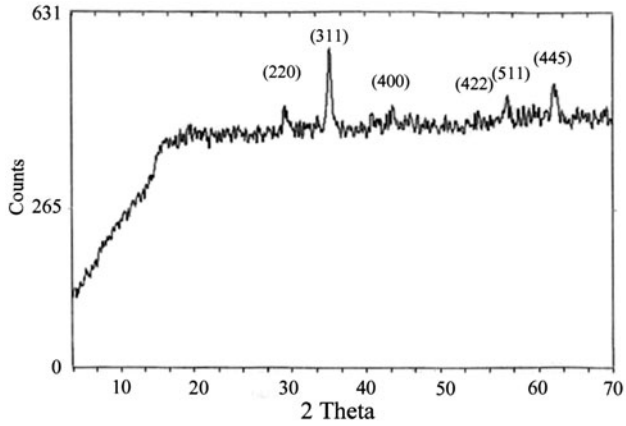

Fig. 4. Powder (XRD) patterns of Fe_3O_4@SiO_2/Schiff base ligand.

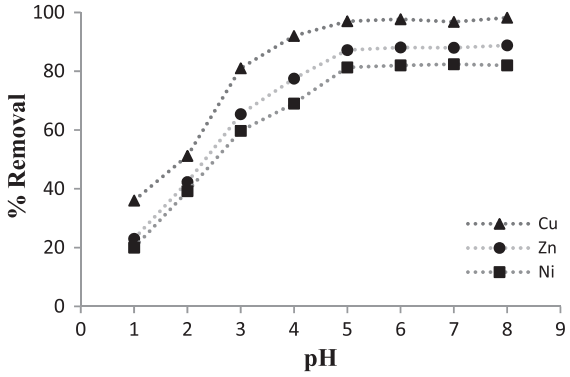

Fig. 5. Effect of pH on the adsorption of metal ions by 50 mg Fe_3O_4@SiO_2/Schiff base ligand (100 ppm and 60 min).

3.4. Effect of contact time and initial heavy metal concentrations

Equilibrium time is one of the important parameters to design a low-cost water treatment system. Fig. 7(a) shows the removal percentage of the metal ions at initial concentration of 100 mg L^{-1} and pH 5. It can be seen that adsorption was rapid initially, and slowed down thereafter, and, finally, reached equilibrium. Therefore, the optimum contact time was considered to be 60 min.

The influence of varying the initial metal ions' concentration was assessed in the range of 25–200 mg L^{-1} (Fig. 7(b)). The mechanism of metal adsorption is in reliance with initial metal ion concentrations. At low concentrations, metals are adsorbed by particular sites, while by further increment of metal ion concentrations, the specific sites are saturated and the exchange sites are filled [23]. Initial concentration provides an important driving force to overcome all mass transfer resistance of the metal ions between the aqueous and solid phases [24].

3.5. Adsorption kinetics

Every adsorption process occurs according to well-known general interaction feature such as chemical reaction, diffusion control, and mass transfer via physical or chemical force. The kinetic parameters benefit the reader for making a prediction to the rate of interpretation and modeling the adsorption processes. The agreement of experimental data and the model-predicted values was expressed by the correlation coefficients (R^2). The closer the theoretical and the experimental values, the better the theoretical model.

The data in Table 1 clearly indicated that the adsorption kinetics better fitted the pseudo-second-order kinetic model, suggesting that the adsorption process was very fast, probably dominated by a chemical adsorption phenomenon. Table 2 shows a comparison of the adsorption capacities of some of the other related adsorbents and this work.

3.6. Adsorption isotherms

The equilibrium adsorption data of Cu(II), Zn(II), and Ni(II) on to Fe_3O_4@SiO_2/Schiff base ligand adsorbent was analyzed using Langmuir and Freundlich models. As shown in Table 2, the R^2 of the Langmuir isotherm was greater than Freundlich isotherms for the adsorption of both investigated metals. According to the assumption of the Langmuir isotherm model, the adsorption of heavy metals onto Fe_3O_4@SiO_2/Schiff base ligand occurred as a monolayer on a

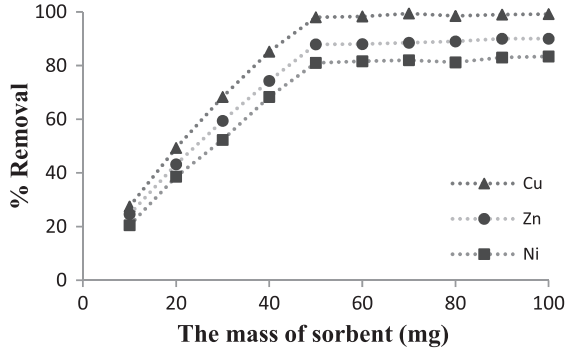

Fig. 6. Effect of dose of Fe_3O_4@SiO_2/Schiff base ligand on the adsorption of Cu(II), Zn(II), and Ni(II) (C_0 = 100 ppm, Time = 60 min, and pH 5).

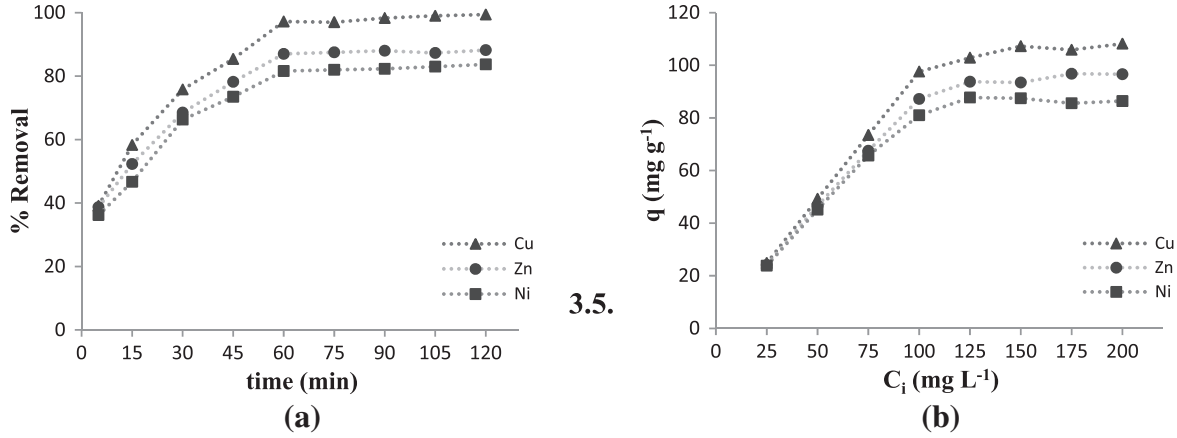

3.5.

Fig. 7. (a) Effect of contact time (100 ppm) and (b) Effect of various initial metal ions concentrations at 60 min, on the adsorption of Cu(II), Zn(II), and Ni(II) onto Fe_3O_4@SiO_2/Schiff base ligand (pH 5, m = 50 mg).

Table 1
Adsorption kinetic data for the removal of Cu(II), Zn(II), and Ni(II) onto Fe_3O_4@SiO_2/Schiff base ligand

Model	Parameter	Cu^{2+}	Zn^{2+}	Ni^{2+}
Pseudo-first-order model	q_e (mg g^{-1})	77.037	58.116	60.939
	K_1 (min^{-1})	0.0462	0.0412	0.0446
	R^2	0.99	0.9905	0.9895
	q_{exp}	97.2	87	81.6
Pseudo-second-order model	q_e (mg g^{-1})	109.89	95.238	91.743
	K_2 (mg (g min)$^{-1}$)	8.33×10^{-4}	11.8×10^{-4}	10.4×10^{-4}
	R^2	0.9977	0.9977	0.997

Table 2
Comparison of adsorption capacities of various adsorbents for metal ions

Type of adsorbent	Adsorption capacities (mg g^{-1})			References
	Zn^{2+}	Cu^{2+}	Ni^{2+}	
Amino-functionalized Fe_3O_4@SiO_2 magnetic nanomaterial	–	30.8	–	[25]
Scrap tire	–	–	25	[26]
Silica gel functionalized with EDTA	–	–	21.6	[27]
Salicylic acid-type chelate adsorbent	31.2	36.9	–	[28]
Copolymer 2-hydroxyethyl methacrylate with monomer methyl methacrylate	–	31.2	–	[29]
Silica-supported dithiocarbamate	–	20.36	–	[30]
Multicarboxyl-functionalized silica gel	39.96	47.07	30.80	[31]
Chitosan-bound Fe_3O_4 nanoparticles	–	21.5	–	[32]
Fe_3O_4 onto tea waste (Fe_3O_4–TW)	–		38.3	[33]
Magnetic maghemite (γ-Fe_2O_3)	84.95	111.11	–	[34]
Fe_3O_4@SiO_2/Schiff base ligand	95.24	109.9	91.74	This work

surface that is homogenous in adsorption affinity. Values of q_m and K_L were calculated from the intercept and slope of the linear plots, respectively, and are presented in Table 3.

Table 3
Adsorption isotherms parameters of Cu(II), Zn(II), and Ni(II) onto Fe_3O_4@SiO_2/Schiff base ligand

Model	Parameter	Cu^{2+}	Zn^{2+}	Ni^{2+}
Freundlich equation				
	K_f	52.856	32.158	28.953
	n	5.128	3.602	3.683
	R^2	0.7533	0.8539	0.8508
Langmuir equation				
	q_m	108.69	100	89.285
	K_L	1.3941	0.3378	0.355
	R^2	0.9998	0.9996	0.9989

4. Conclusion

The present work showed that Fe_3O_4@SiO_2/Schiff base ligand was considerably efficient to remove heavy metals from aqueous solutions. The adsorption was highly dependent on contact time, adsorbent dosage, initial heavy metal concentration, and pH. The most ideal pH value to adsorb heavy metals was 5. The kinetics of heavy metals adsorptions on adsorbent followed the pseudo-second-order model. The equilibrium data fitted well in the Langmuir model of adsorption, showing monolayer coverage of heavy metals molecules at the outer surface of Fe_3O_4@SiO_2/Schiff base ligand. The value for the maximum adsorption capacity, q_m, was comparable with the values for commercial adsorbent reported in earlier studies.

Acknowledgments

The authors express their sincere thanks to the authorities of Semnan University for financing the project.

References

[1] D.E. Salt, R.D. Smith, I. Raskin, Phytoremediation, hand-book-of-plant-growth-pH ann, Rev. Plant Physiol. Plant Mol. Biol. 49 (1998) 643–668.
[2] (a) A. Olad, S. Ahmadi, A. Rashidzadeh, Removal of nickel (II) from aqueous solutions with polypyrrole modified clinoptilolite: Kinetic and isotherm studies, Desalin. Water Treat. 51 (2013) 7172–7180. (b) S.K. Bozbas, U. Ay, A. Kayan, Novel inorganic–organic hybrid polymers to remove heavy metals from aqueous solution, Desalin. Water Treat. 51 (2013) 7208–7215.
[3] S.O. Yong, J.E. Yang, Y.S. Zhang, S.J. Kim, D.Y. Chung, Heavy metal adsorption by a formulated zeolite–Portland cement mixture, J. Hazard. Mater. 147 (2007) 91–96.
[4] A. Wdjtowicz, A. Stokμosa, Removal of heavy metal ions on smectite ion-exchange column, Pol. J. Environ. Stud. 11(1) (2002) 97–101.
[5] V.C. Taty-Costodes, H. Fauduet, C. Porte, A. Delacroix, Removal of Cd (II) and Pb (II) ions, from aqueous solutions, by adsorption onto sawdust of *Pinus sylvestris*, J. Hazard. Mater. B105 (2003) 121–142.
[6] G. Tiravanti, D. Petruzzelli, R. Passino, Pretreatment of tannery wastewater by an ion exchange process for Cr(III) removal and recovery, J. Water Sci. Technol. 36 (1997) 197–207.
[7] S. Rengaraj, C.K. Joo, Y. Kim, J. Yi, Kinetics of removal of chromium from water and electronic process wastewater by ion exchange resin, J. Hazard Mater. 102 (2003) 257–275.
[8] D. Petruzzelli, R. Passino, G. Tiravanti, Ion exchange process for chromium removal and recovery from tannery wastes, J. Ind. Eng. Chem. Res. 34 (1995) 2612–2617.
[9] Q. Peng, Y. Liu, G. Zeng, W. Xu, Biosorption of copper(II) by immobilizing *Saccharomyces cerevisiae* on the surface of chitosan-coated magnetic nanoparticles from aqueous solution, J. Hazard. Mater. 177 (2010) 676–682.
[10] S.S. Banerjee, D. Chen, Fast removal of copper ions by gum Arabic modified magnetic nano-adsorbent, J. Hazard. Mater. 147 (2007) 792–799.
[11] M.H. Mashhadizadeh, Z. Karami, Solid phase extraction of trace amounts of Ag, Cd, Cu, and Zn in environmental samples using magnetic nanoparticles coated by 3-(trimethoxysilyl)-1-propantiol and modified with 2-amino-5-mercapto-1,3,4-thiadiazole and their determination by ICP-OES, J. Hazard. Mater. 190 (2011) 1023–1029.
[12] H. Shaalan, M. Sorour, S. Tewfik, Simulation and optimization of a membrane system for chromium recovery from tanning wastes, Desalination 141 (2001) 315–324.
[13] C.A. Kozlowski, W. Walkowiak, Removal of chromium (VI) from aqueous solutions by polymer inclusion membranes, J. Water Res. 36 (2002) 4870–4876.
[14] S.H. Huang, D.H. Chen, Rapid removal of heavy metal cations and anions from aqueous solutions by an amino-functionalized magnetic nano-adsorbent, J. Hazard. Mater. 163 (2009) 174–179.
[15] N. Kongsricharoern, C. Polprasert, Chromium removal by a bipolar electrochemical precipitation process, J. Water Sci. Technol. 34 (1996) 109–116.
[16] M.H. Liao, D.H. Chen, Fast and efficient adsorption/desorption of protein by a novel magnetic nano-adsorbent, Biotechnol. Lett. 24 (2002) 1913–1917.

[17] M.H. Liao, D.H. Chen, Preparation and characterization of a novel magnetic nano-adsorbent, J. Mater. Chem. 12 (2002) 3654–3659.
[18] N. Raman, Y.P. Raja, A. Kulandaisamy, Synthesis and characterisation of Cu(II), Ni(II), Mn(II), Zn(II) and VO(II) Schiff base complexes derived fromo-phenylenediamine and acetoacetanilide, J. Chem. Sci. 113 (2001) 183–189.
[19] C.T. Barboiu, M. Luca, C. Pop, E. Brewster, M.E. Dinculescu, Carbonic anhydrase activators, part 14: Syntheses of mono and bis pyridinium salt derivatives of 2-amino-5-(2-aminoethyl)- and 2-amino-5-(3-aminopropyl)-1,3,4-thiadiazole and their interaction with isozyme II, Eur. J. Med. Chem. 31 (1996) 597–606.
[20] H. Keypour, M. Rezaeivala, L. Valencia, P. Pérez-Lourido, H.R. Khavasi, Synthesis and characterization of some new Co(II) and Cd(II) macroacyclic Schiff-base complexes containing piperazine moiety, Polyhedron 28 (2009) 3755–3758.
[21] M. Rajabi, S. Asemipour, B. Barfi, M.R. Jamali, M. Behzad, Ultrasound-assisted ionic liquid based dispersive liquid–liquid microextraction and flame atomic absorption spectrometry of cobalt, copper, and zinc in environmental water samples, J. Mol. Liq. 194 (2014) 166–171.
[22] A. Asghari, M. Ghazaghi, M. Rajabi, M. Behzad, M. Ghaedi, Ionic liquid-based dispersive liquid–liquid microextraction combined with high performance liquid chromatography–UV detection for the simultaneous pre-concentration and determination of Ni, Co, Cu and Zn in water samples, J. Serb. Chem. Soc. 79 (2014) 63–76.
[23] P. Salehi, B. Asghari, F. Mohammadi, Removal of heavy metals from aqueous solutions by Cercis siliquastrum L, J. Iran. Chem. Soc. 5 (2008) 80–86.
[24] M.H. Karaoglu, M. Dogan, M. Alkan, Kinetic analysis of reactive blue 221 adsorption on kaolinite, Desalination 256 (2010) (2010) 154–165.
[25] J. Wang, S. Zheng, Y. Shao, J. Liu, Z. Xu, D. Zhu, Amino-functionalized Fe_3O_4@ SiO_2 core–shell magnetic nanomaterial as a novel adsorbent for aqueous heavy metals removal, J. Colloid Interface Sci. 349 (2010) 293–299.
[26] V.K. Gupta, Suhas, A. Nayak, Sh. Agarwal, M. Chaudhary, I. Tyagi, Removal of Ni(II) ions from water using scrap tire, J. Mol. Liq. 190 (2014) 215–222. Available from: http://www.sciencedirect.com/science/article/pii/S0167732213003711.
[27] E. Repo, T.A. Kurniawan, J.K. Warchol, M.E.T. Sillanpää, Removal of Co(II) and Ni(II) ions from contaminated water using silica gel functionalized with EDTA and/or DTPA as chelating agents, J. Hazard. Mater. 171 (2009) 1071–1080.
[28] F. An, B. Gao, X. Dai, Efficient removal of heavy metal ions from aqueous solution using salicylic acid type chelate adsorbent, J. Hazard. Mater. 192 (2011) 956–962.
[29] O. Moradi, M. Aghaie, K. Zarea, M. Monajjemi, H. Aghaiea, The study of adsorption characteristics Cu^{2+} and Pb^{2+} ions onto PHEMA and P(MMA-HEMA) surfaces from aqueous single solution, J. Hazard. Mater. 170 (2009) 673–679.
[30] L. Bai, H. Hu, W. Fu, Synthesis of a novel silica-supported dithiocarbamate adsorbent and its properties for the removal of heavy metal ions, J. Hazard. Mater. 195 (2011) 261–275.
[31] M. Li, M. Li, Ch. Feng, Q. Zeng, Preparation and characterization of multi-carboxyl-functionalized silica gel for removal of Cu(II), Cd(II), Ni(II) and Zn(II) from aqueous solution, Appl. Surf. Sci. 314 (2014) 1063–1069.
[32] Y.C. Chang, D.H. Chen, Preparation and adsorption properties of monodisperse chitosan-bound Fe_3O_4 magnetic nanoparticles for removal of Cu(II) ions, J. Colloid Interface Sci. 283 (2005) 446–451.
[33] P. Panneerselvam, N. Morad, K.A. Tan, Magnetic nanoparticle (Fe_3O_4) impregnated onto tea waste for the removal of nickel(II) from aqueous solution, J. Hazard. Mater. 186 (2011) 160–168.
[34] A. Roy, J. Bhattacharya, Removal of Cu(II), Zn(II) and Pb(II) from water using microwave-assisted synthesized maghemite nanotubes, Chem. Eng. J. 211–212 (2012) 493–500.